Resonant Angle-Resolved Photoemission of URu_2Si_2

J. D. Denlinger[1], G.-H. Gweon[1], J. W. Allen[1], C. G. Olson[2], Y. Dalichaouch[3], B. W. Lee[3], M. B. Maple[3], P. E. Armstrong[4], and Z. Fisk[5]

[1]Department of Physics, University of Michigan, Ann Arbor, Michigan 48109, USA
[2]Iowa State University/Ames Laboratory, Ames, Iowa 50011, USA
[3]Department of Physics, University of California at San Diego, La Jolla, California 92093, USA
[4]Los Alamos National Laboratory, Los Alamos, New Mexico 87545, USA
[5]NHMFL, Florida State University, Tallahassee, Florida 32306, USA

INTRODUCTION

Heavy fermion compounds are characterized by a large linear specific heat coefficient (γ) which signals large ('heavy') effective masses of electrons forming the Fermi surface [1]. Resonant photoemission spectroscopy of polycrystalline samples has contributed to the understanding of rare earth and actinide heavy fermions by identification of the *f*-electron weight contribution to the states at E_F For many rare earth systems this weight can be analyzed and related to γ within a single impurity picture [2, 3]. Nonetheless from general theoretical ideas [4] and early experimental de Haas-van Alphen studies [5] it has been appreciated for very many years that this weight should be part of the dispersions which define the Fermi surface. One finds that issues concerning the band width and dispersion of this *f*-weight and the appropriate starting point (single-impurity models versus band-theory) for the theoretical description of various heavy fermion materials are commonly raised in the literature [6]. High-resolution angle-resolved photoemission spectroscopy (ARPES) of single crystal surfaces holds largely unfullfilled promise for addressing these issues.

The goal of this work is to carefully quantify the variation of *f*-weight of the heavy fermion URu_2Si_2 as a function of crystal momentum by combining ARPES with resonant photoemission at energies near the U $5d \rightarrow 5f$ absorption threshold. URu_2Si_2 has a moderately large linear specific heat coefficient of $\gamma \sim 65$ mJ/mol-K^2 [7] compared to ~1 for a simple metal and >1500 for $CeAl_3$. URu_2Si_2 is a paramagnet that undergoes antiferromagnetic ordering at 17.5 K and then becomes superconducting at 1.2 K [8]. Additional interest in this material is due to evidence for the coexistence of antiferromagnetism and superconductivity, properties generally thought to be mutually exclusive. Also, the Ce analog to this compound, $CeRu_2Si_2$, is well-known in the literature for excellent agreement between de Haas-van Alphen measurements and renormalized band theory, i.e. the number, size and effective masses of Fermi surface orbits well account for its T-linear specific heat value of ~350 [9].

EXPERIMENT

URu_2Si_2 has the $ThCr_2Si_2$ crystal structure and a body-centered tetragonal Brillouin zone. Samples were cleaved in ultra-high vacuum (1.2×10^{-10} torr) at room temperature exposing the [001] surface and then cooled to ~150 K for ARPES measurements. Crystals with a ~3 mm diameter typically produced at least one ~1 mm^2 flat uniform terrace suitable for analysis. ARPES experiments were performed on the ALS Beamline 7.0.1.2 with an experimental endstation originally designed for highly-automated angular and energy-dependent photoelectron diffraction. The inherent motion of the beam on the sample surface with sample rotation presented an experimental challenge to keep the 100 μm beam spot on the millimeter-sized uniform cleave terraces. A total instrumental resolution of ≈80 meV and full angular acceptance of ≈1.4° (10% of a Brillouin zone width) was employed. These ARPES measurements in the photon energy range of 80-220 eV complement previous lower photon energy measurements (14-34 eV) performed at the SRC synchrotron in Wisconsin.

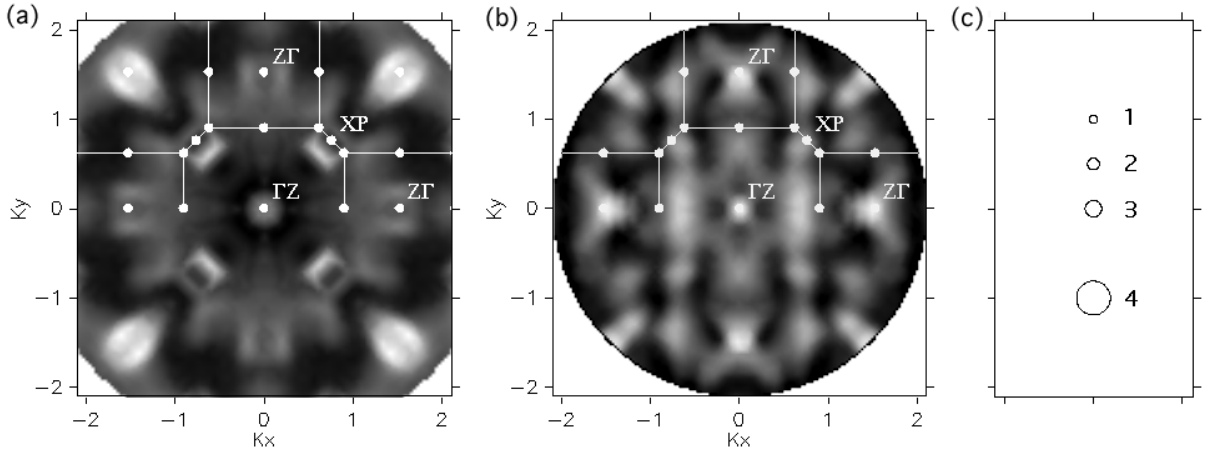

Figure 1. Fermi-edge intensity angular maps of URu_2Si_2 (001) at two photon energies, (a) 85 eV and (b) 112 eV, below and above the U 5*f* resonance. (c) Representative sizes of Fermi-surface orbits measured by magnetoresistance.

RESULTS

Figure 1 shows Fermi-edge angular intensity maps for two photon energies below and above the U $5d \rightarrow 5f$ resonance. The maps are acquired by monitoring the intensity within a 0.2 eV wide energy window centered on E_F while the sample is rotated over a 45° or 90° azimuth range out to a maximum polar angle of 25°. The full azimuth images, obtained by symmetrization, represent curved surfaces in *k*-space and are plotted versus *k*-parallel with a partial Brillouin zone overlaid for reference. Below resonance (85 eV) the most distinct Fermi surface feature is a ring structure centered on XP. In addition, intensity maxima are observed at ΓZ at normal emission and in the second Brillouin zones. Above resonance (112 eV), strong intensity modulation of the U 5*f* weight is observed with maxima along ΓZ and approximately half-way between Γ and Z. Additionally, the XP ring structure is observed to fill in with *f*-weight.

The origin of the E_F intensity modulations is investigated with angle-resolved spectra at the Γ, Z, X and M *k*-points as displayed in Figure 2. The Γ-point spectra along normal emission at 97 eV (Fig. 2a) shows a sharp peak near E_F that is measured to have a finite binding energy at lower photon energy (18 eV). In addition, the build-up of weight at 0.6 eV is a key signature of the

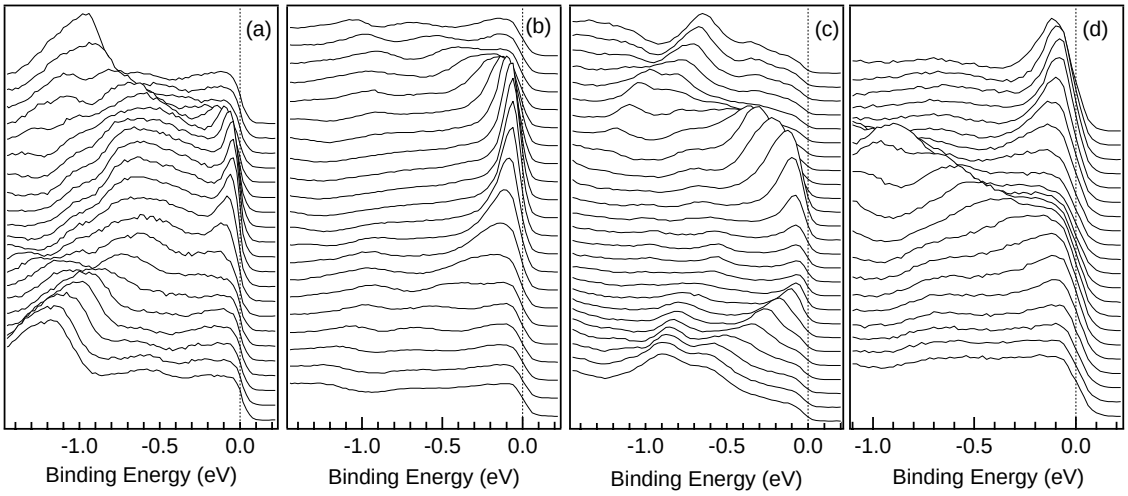

Figure 2. Major Fermi surface regions in k-space: (a) small hole pocket at Γ (97 eV), (b) tiny hole pocket at Z (125 eV), (c) medium-sized hole surface at X (85 eV), and (d) a large electron-like dispersion centered on Γ (156 eV).

Γ-point that repeats as a function of photon energy (18, 50, 97, 156 and 220 eV) and allows the determination of a crystal inner potential (V_0=12 eV) that sets the k_z-scale for all measurements. In contrast, this 0.6 eV binding energy weight is absent at the Z-point at normal emission at 125 eV. The sharp dispersive weight at E_F at Z is shown at low photon energy to be a tiny hole surface. The XP-point ring structure, Fig. 2c, is observed to be a small hole-surface. As a function of photon energy the intensity of this ring is observed to form a tube of intensity. This tube structure is believed to originate from an ellipsoidal Fermi surface centered on the X or P points and then k_z-broadened as a result of the finite inelastic mean-free path of the outgoing electron. Finally a larger electron-like surface becomes very distinct in the spectra at 156 eV, Fig. 2d, and probably accounts for the E_F intensity maxima halfway between Γ and Z in Fig. 1b.

ANALYSIS

Meaningful comparison of band dispersions along short polar arcs near normal emission can be made to calculated band structures for URu_2Si_2 [10-12]. An intensity representation of such a polar series at 156 eV is shown in Fig. 3a in which image normalization and enhancement has been employed to bring out the weaker band features at higher binding energy. The experimental band dispersions are digitized and overplotted (dots) in Fig. 3b with a calculated band structure along ΓMZ [12]. Good agreement is observed in the higher binding energy (*d*-band) dispersions. In particular the symmetric dispersion to a maximum binding energy of 1.5 eV between Γ and Z and the close approach of the hole-like dispersion at Z are well reproduced. In addition, the band edge energies at Γ are in good agreement with calculations.

However, in the near E_F region there is significant disagreement with theory. A small theoretical electron surface at Γ is predicted instead the observed hole-like dispersion and the large electron-like dispersion centered on Γ has no correspondence in the band theory. In addition, the various band calculations predict none or a small electron surface at X (not shown) in contrast to the observed medium-sized hole surface along XP. The discrepancy between the calculated and experimental Fermi surface topology is also exhibited in quantum oscillation measurements [13, 14]. Four orbits are observed in magnetoresistance [14] whose cross sectional areas are illustrated in Fig. 1c, plotted with the same k-parallel scale as the E_F intensity maps. The largest orbit with a frequency of 1.1 kT is qualitatively observed to match well with the XP ring structure. Also the small hole surface at Z is a candidate to match one or two of the smaller orbits. Effective

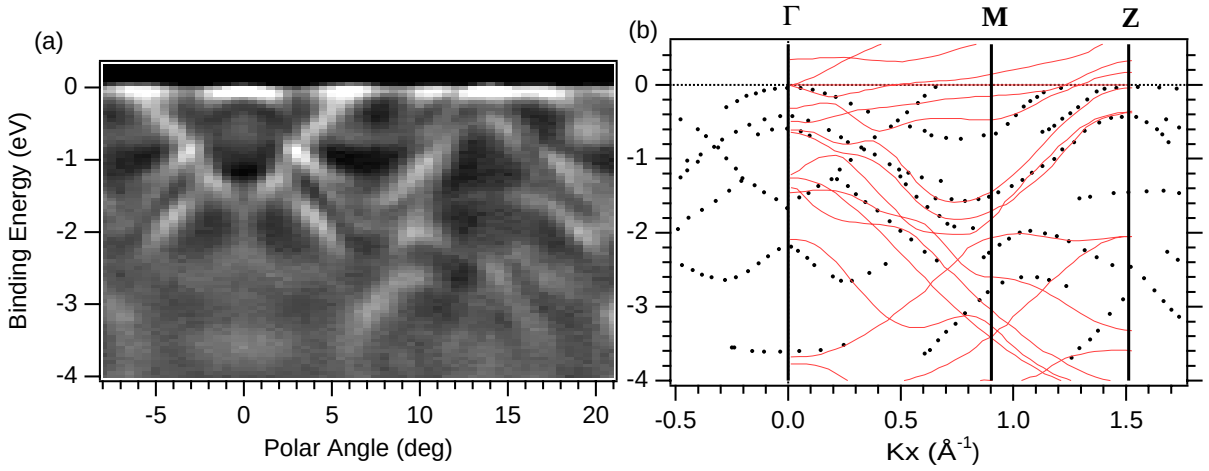

Figure 3. (a) Normalized intensity plot of polar series of spectra along [100] at [156 eV. (b) Comparison of experimental (dots) bands to calculated band structure along ΓMZ (lines).

masses of 6-12 m_e are measured for these orbits and are not sufficiently large to fully account for the 65 mJ/mol-K^2 linear specific heat coefficient. The topology of the large electron surface, Fig. 2d, has not been quantified, but if spherical, it would correspond to a 13 kT oscillation frequency.

The discrepancy between relativistic band calculations and measurements of ARPES and magnetoresistance can be attributed to many body effects. The relativistic calculations treat three U 5*f*-electrons as part of the valence band without any correlation between *f*-electrons. Renormalized band theory, not performed to date for URu_2Si_2, empirically modifies the *f*-electron scattering phase shifts in order to account for correlations resulting in much flatter *f*-bands and hence larger Fermi-surface effective masses. In the case of $CeRu_2Si_2$ and UPt_3, the Fermi surface is only slightly modified after renormalization. An alternate theoretical approach is to start with the single-impurity Anderson description of *f*-electron correlations and add lattice effects [15]. Signatures of this periodic Anderson model include renormalization of the bare *f*-binding energy to just above E_F, and *f*-*d* mixing in the vicinity of a *d*-band crossing E_F. The observed dispersion and rapid loss of intensity of the sharp *f*-weight away from E_F (Fig. 2) is currently being analyzed in terms of this many-body model *f*-*d* band mixing.

REFERENCES

1. G. R. Stewart, Rev. Mod. Phys. **56**, 755 (1984).
2. J. W. Allen, *et al*., Adv. Phys. **35**, 275 (1986).
3. D. Malterre, M. Grioni, and Y. Baer, Adv. Phys. **45**, 299 (1996).
4. R. M. Martin, Phys. Rev. Lett. **48**, 362 (1982).
5. W. R. Johanson, *et al*., Phys. Rev. Lett. **46**, 504 (1981).
6. see for example, A. J. Arko, *et al*., J. Alloys Compd. **271-3**, 826 (1998).
7. M. B. Maple, *et al*., Phys. Rev. Lett. **56**, 185 (1986).
8. T. T. M. Palstra, *et al*., Phys. Rev. Lett. **55**, 2727 (1985).
9. G. Zwicknagl, Adv. Phys. **41**, 203 (1992).
10. M. R. Norman, T. Oguchi, and A. J. Freeman, Phys. Rev. B **38**, 11193 (1988).
11. G. J. Rozing, P. E. Mijnarends, and D. D. Koelling, Phys. Rev. B **43**, 9515 (1991).
12. H. Yamagami, (private communication, 1998).
13. C. Bergemann, Master's Thesis (Cambridge, 1996).
14. N. Kellar, *et al*., J. Magn. Magn. Mater. **177-181**, 298 (1998).
15. A. N. Tahvildar-Zadeh, M. Jarrell, and J. K. Freericks, Phys. Rev. Lett. **80**, 5168 (1998).

This work was supported by the U.S. Dept. of Energy (DoE) under contract No. DE-FG02-90ER45416 and by the U.S. NSF under grant No. DMR-94-23741.

Principal investigator: Jonathan Denlinger, Department of Physics, University of Michigan. Email: JDDenlinger@lbl.gov. Telephone: 510-486-5648.